Sensor Placement Optimisation Strategies on Beams for Structural Health Monitoring Applications

Wishawin Lertnawapan

Supervised by Dr. Sergio Cantero Chinchilla

Bachelor of Mechanical Engineering

School of Electrical, Electronic, and Mechanical Engineering

University of Bristol

May 2024

Declaration

This project report is submitted towards an application for a degree in Mechanical Engineering at the University of Bristol. The report is based upon independent work by the candidate. All contributions from others have been acknowledged and the supervisor is identified on the front page. The views expressed within the report are those of the author and not of the University of Bristol.

I hereby assert my right to be identified as the author of this report. I give permission to the University of Bristol Library to add this report to its stock and to make it available for consultation in the library, and for inter-library lending for use in another library. It may be copied in full or in part for any bona fide library or research worker on the understanding that users are made aware of their obligations under copyright legislation.

I hereby declare that the above statements are true.

Abstract

A comparison of state-of-the-art Sensor Placement Optimisation (SPO) strategies applied to structural beams and recommendation for practical sensor layouts. Vibration-based Damage Detection (VDD) is a popular methodology within Structural Health Monitoring (SHM), resolving damage within a structure by identifying changes in ambient vibration properties, often by comparison with control data. The paper retrieves numerical flexural vibration data of low-frequency modes and natural frequencies using a Finite Element (FEA) model of a beam. Two common beam constraints were considered in the cantilever and the en-castre beam. Five objective functions and three optimisation algorithms (OA) were compared to formulate a set of potential Optimal Sensor Layouts (OSL); subsequent performance evaluation for each based on the OSL itself, convergence studies, and resilience to artificial noise. The outcome shows DE is the best OA for beam optimisation and problems of similar dimensionality. Effective-Independence Driving Point Residue (EI-DPV) and Eigenvalue Vector Product (EVP) observed the best performance in the cantilever and fixed beam cases, respectively. On a 100-element beam, six sensors are proposed to be positioned on nodes [32,45, 56, 62, 68, 83] and [17, 30, 43, 57, 70, 83] respectively. Validation was performed on an FEA model, using artificial damage by stiffness reduction at specific sections. Results of this study conclude that EIDPV/DE and EVP/DE OSLs can identify the presence of structural damage (Class I); however, are unable to quantitively state or localise stiffness-reduced regions along the beam (Class II).

Contents

1 Introduction

1.1 Background

Structural steel beams are critical in various industrial applications in modern infrastructure as load-bearing components. In recent decades, through repeated loading, these structures have been subject to decay and are prone to fatigue. A study conducted by the Committee of American Society of Civil Engineers (ASCE) showed that 80-90% of failures in steel structures are related to continuous local damage accumulation under the structural capacity[1]. Many studies currently approach uniform beams for design and deflection calculations, with limited damage identification methods[2]. Thus, it is important to find cost-effective solutions for early damage detection with the goal of preventing failure, reducing maintenance investments and ensure the sustainability of structures through autonomous monitoring. Advances in Structure Health Monitoring (SHM) address these shortcomings, providing innovative methods to monitor and assess the integrity of a structure more efficiently or where classic local inspection is difficult or impossible[3].

The principles of SHM involve periodic monitoring of a structure, for which acquired data may have distinct, identifiable characteristics between damaged and undamaged structures[10]. Brownjohn[4] and Karbhari et al.[5] discussed the motivations behind SHM for different civil structures. This field is increasingly extensive, and the design of an SHM is heavily influenced by a multitude of factors and their intended applications. An ideal SHM should be cost-effective, sensitive to low damage levels, and resilient to noise. Additionally, SHM systems will vary largely by the objectives of the structure to be installed and potential restrictions. An example guideline includes considerations of i) the monitoring scale, ii) the method, iii) the period, and iv) damage classification. The latter comprises four levels: Class I: Damage detection; Class II: Localization; Class III: Quantification; Class IV: Evolution and Prognosis[6]. The current state of the art within SHM is primarily within Class II detection[18] with some successful techniques, including Vibration-based, Strain-based, and Wave-based monitoring[78].

Vibration-based damage detection (VDD) is among the earliest proposed identification strategies pioneered by Adams et. Al[9],. Many VDD methods have been developed for aerospace, civil, and mechanical uses[22]. VDD is a form of non-destructive testing which attributes damage detection and identification by resolving a change in a structure's structural properties, which alters as it responds to dynamic perturbations, with the methodology investigated by Frigui et al. on a finite element model[6,10]. Svendsen et al. investigated the utilisation of VDD data to evaluate the condition at a global scale[11], with landmark contributions by Kammer[15]. A recent review on dynamic-based SHM can be found in Gopalakrishnan et al[12]. To obtain this data for SHM, a sensor network may be constructed. This leads to the question of sensor distribution, posing the question of where sensors should be placed within the network.

It is impractical – sometimes impossible – to place sensors in all locations of a structure. Thus, the layout must evaluate the positions of most information while maintaining complete data. Such methods have been developed to compute solutions and are collectively referred to as Sensor Placement Optimisation (SPO), first conceptualised in engineering applications by Padula et al.[13]. SPO is currently growing as a field of research interest; however, only 4.5% of SHM papers investigate this area. Hence, there is a necessity for continued studies[18]. By optimising SPO, SHM systems can be improved to reduce unnecessary maintenance costs due to false negatives, and solutions to data management challenges may be explored[14].

Fundamentally, SPO is limited by the number of sensors available to the sensor network. This configuration of sensors – referred to as the Optimal Sensor Layout (OSL), will be suboptimal. However, the layout should ideally be sufficient to represent the system and perform SHM without compromising accuracy[10]. Generally, SPO can be reduced as a standard optimisation problem through the minimisation of an objective function based on the system's internal parameters. Illustrated in equation 1, an optimum subset of sensor locations S can be obtained given a candidate set of target modes[15].

$$\begin{gathered} \min f(S), \text{ for } |\{S \in \mathbb{Z}^+, n\}| = D \\ \text{for } f: \mathbb{R}^n \rightarrow \mathbb{R} \\ : \begin{cases} g_i(S) \leq 0 & \forall \quad i = 1, \dots, m \\ h_i(S) = 0 & \forall \quad i = 1, \dots, p \end{cases} \end{gathered} \tag{1}$$

[1] (Y.Q. Ni, Ye, & J.M. Ko, 2010)
[2] (K. Yeh, 1988)
[3] (G.F. Gomes, 2018)
[4] (Brownjohn, 2007)
[5] (V.M. Karbhari, 2009)
[6] (F. Frigui, 2018)
[7] (X. Ye, 2012)
[8] (B. Shi, 2022)
[9] (R.D. Adams, 1978)
[10] (S. Hassani U. D., 2023)
[11] (B.T. Svendsen, 2022, Vol.12)
[12] (S. Gopalakrishnan, 2011)
[13] (S. Padula, 1998)
[14] (S. Mustapha, 2021)
[15] (Kammer, 1991)

where D is the number of sensors to optimise by minimising the objective function, f; in which all inequality constraint functions $h(S)$ and equality constraint functions $g(S)$ are satisfied[16]. The range for which S exists lies within a defined solution space of size n.

Since 1940, significant effort has been placed into the development of algorithms to solve optimisation problems, in which the effectiveness varies considerably depending on various factors[16]. The standard approach of SPO within an appropriate SHM can be outlined by the following:

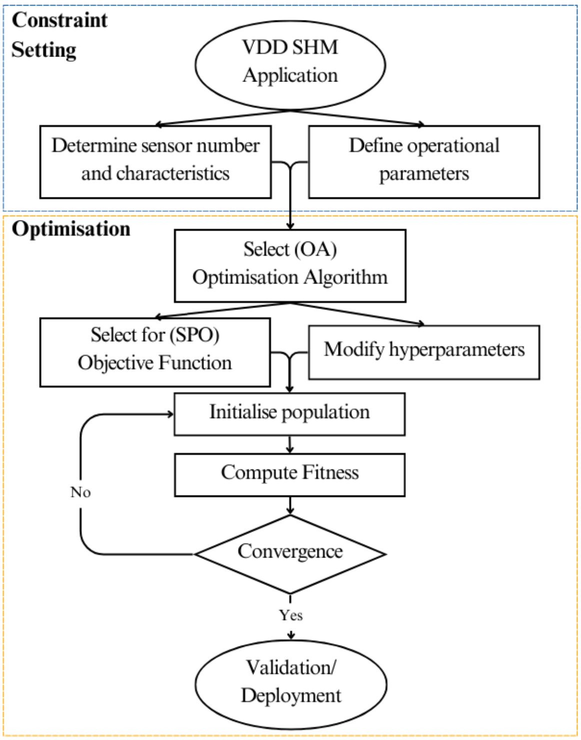

Figure 1 – SPO Framework[10]

Additionally, factors must be considered to select appropriate sensor characteristics, namely sensor type, cost, installation, and environmental sensitivity. The number of sensors considered should directly correspond to the number of modes of interest. As it is common practice for SPO systems to align the number of translational Degrees of Freedom (DOF) of a structure to the possible candidate modes, the two are often referred to interchangeably[10], thus the number of sensors must be less than or equal to the modes to be identified[72]. The nature of environmental noise must be accounted for as the type of external influence the monitored structure is likely to experience, including temperature, acoustic, and electromagnetic interferences. SHM systems have incorporated a wide range of sensor types which collect unique measurement types. Most commonly, displacement and acceleration measurements are used, though strain, force, and local pressure data have been performed in the literature; as sensor technology over the past several years for this application has been developed, many recent papers have drawn towards using advanced sensor types such as piezoresistive and fibre optics A more extensive review can be found by Hassani et al.[23]

Using several methodologies, the performance of a given sensor layout is quantified by applying various metrics as part of the optimisation problem's function. As such, these methods are often referred to as objective functions (see Section 3). Defining and evaluating metric performances with respect to each optimisation method is highly problem-dependent, and as such, the results of this study may only be relevant to SPO for this scenario.

1.2 Aims

This paper aims to compare various applied strategies in current literature for the optimisation of sensor placements by application of multiple objective functions and optimisation algorithms (OAs), following the flowchart of SPO as outlined in Figure 1[26], and as a contribution following the research of Panigrahi[77] and Civera et al.[17] . More specifically, the comparison of these various strategies in the context of damage detection within beams subject to two different boundary conditions – with one restricted end along all degrees of freedom, i.e. a cantilever beam[18]; and with both ends fixed, i.e. an en-castre or bounded beam. These cases were chosen as the most commonly found loading arrangements as part of structures.

[16] (Boyd & Bandenberghe, 2004)

[17] (M. Civera, 2021)

Considering the SHM guidelines in Section 1.1, Long-term monitoring was deemed a rational monitoring period as the objective of this study is within the context of low-cost optimisation. Damage classification is limited to Class I[18] as it is impractical to incorporate higher classes autonomously within the sensor network when it can be assumed the presence of damage detection will likely lead to an immediate inspection. However, Class II will be attempted.

To further limit the extent of content covered, only modal displacement and natural frequency data vibration data are collected under the case of pure flexural bending modes. These are examples of ambient vibration data, retrieving information through the change of the structure's intrinsic properties. Modal analysis was preferred, as it is one of few non-destructive methods applicable to global structures, as opposed to newer strategies such as ultrasonic and X-ray techniques where localisation cannot be guaranteed[19]. Modal Assurance Criterion (MAC)[17], Coordinate Modal Assurance Criterion (COMAC) are popular statistical methods developed by Allemang[20]. Other methods exploit Modal Curvature (MCM) by Pandey et al.[21]; strain energy; curvature (CDF); flexibility ; or damping[23,6]. Using modal displacement and natural frequency in tandem is a standard metric in VDD due to their reliability and ease of acquisition, which can be exploited to detect and locate damage[22], using lower frequency data and are used to characterise global behaviour[23]. The decision to collect both sets of data types is a common approach to ensure validity. As cited, modal data is more sensitive, which allows minor effects to be detected; however, it can lead to interference from environmental noise[24]. Natural frequencies, in contrast, are less sensitive, mitigating the drawbacks of modal information, but are unable to differentiate symmetric and minute structural faults.

For the application of a cantilever beam under which this combination of data is accessible, only the first six modes are considered to determine a unique convergence solution to the optimisation accurately[25,26]. Multiple sensor measurement types can be used to formulate modal and natural frequency data. As it is not the subject of the paper, all data is assumed to be collected by highly sensitive sensors in noiseless conditions.

Data was acquired using Finite Element Analysis (FEA) on an undamaged model using Abaqus™ software (see section 2) under two boundary conditions. This data is then subject to five different objective functions to map a given candidate location in the form of an output information function. Three OAs were simulated to calculate the extrema of each information function to extract the six sensor locations. As no benchmark assessment standards do not appear to exist in the literature[38], subsequent evaluation of each pair of strategies was done by investigating three metrics:

1. The resulting optimal sensor layout
2. Convergence behaviour, such as rate and reliability of convergence of the population's best and average
3. Performance under environmental noise

Due to the inherent stochasticity present in the OAs (Section 4), results of optimisation will vary; several runs were performed and then averaged to ensure fair comparison.

For each beam configuration, an objective function/OA pair was selected as the best-performing strategy based on the criteria outlined. By introducing a form of damage in an FEA model, an example of validation was conducted by determining the significance of the changes in the recorded modal data using the selected OSL and whether Class I and Class II damage identification can be ascertained.

2 Data Acquisition

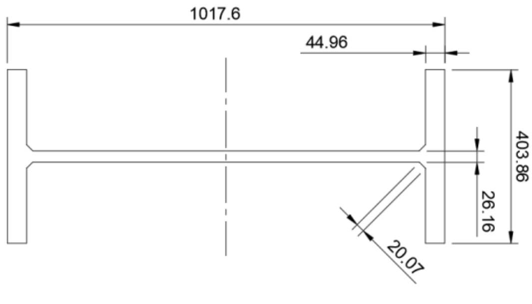

Figure 2 – Dimensions for the W44x335 section in mm

A wide range of structural steel dimensions and geometries are used in structures to serve as primary weight-bearing components. "Beams" are components standardised by AISI into one of three geometries: S, W, and H[27]. This study aims

[18] (W. Ostachowicz, 2019)
[19] (W. Fan, 2011)
[20] (Allemang, 1982)
[21] (A. Pandey, 1991)
[22] (Cawley & Adams, 1979)
[23] (S. Hassani M. M., Structural Health Monitoring in Composite Structures: A Comprehensive Review, 2022)
[24] (C.R. Farrar, 1997)
[25] (Krishnanunni, 2019)
[26] (H. Hao, 2002)
[27] (Thomas Industry, 2022)

to generalise OSL to the most extreme application of such components. The American Institute of Steel Construction (AISC) W44x335 was referred to as the largest standard commercial beam, with a length of 100m and geometric parameters displayed in Figure 2.

An analytical solution to uniform beams subject to pure elastic bending can be ascertained through Euler-Bernoulli linear static analysis governed by equation 2:

$$\frac{d^4y}{dx^4} + \frac{\rho A(x)}{EI(x)}\left(\frac{\partial^2 y}{\partial t^2}\right) = 0 \qquad (2)$$

In which y represents the vertical displacements, a mode shape and its derivatives are formulated with respect to the axial distance along the beam, x, and time t. Other material and geometric properties encoded include density ρ, Young's Modulus E, sectional area A, and second moment of area, I.

However, obtaining frequency data numerically using FEA was a preferred alternative over using analytical methods as it was significantly more time efficient to an acceptable degree of accuracy. The FEA model was generated on Abaqus™, using material properties as specified in section 2.1. A beam was generated using the section dimensions outlined in Figure 2 and ASTM A36 steel material parameters – being the most common structural steel in infrastructure[27]. Several approaches towards this were considered. Initial models attempted to extrude the solid beam from a planar section; however, in all cases, they experienced combined loading from torsional and axial vibrations, which proved difficult to isolate. Using an oriented wire beam from a linear beam element (B31OS) with a defined I-beam section omitted the torsional components and reduced the dimension of the problem but retained axial vibration modes, leading to degenerate modes with no vertical displacement[28]. This was eventually resolved by using a combination of encastre and displacement-constrained boundary conditions for all degrees of freedom at the ends.

Using a global element seed size of 1 ensured mesh nodes intersected along integer values of the beam, allowing all degrees of freedom to be assigned directly to the set of the solution space n for the optimisation problem presented in equation 1.

As a linear system, both forms of frequency information can be extracted through modal superposition procedures[28]. A single-step Lanczos-based linear perturbation analysis was conducted to obtain the first six modes and their respective eigenfrequencies and mode shapes. Figure 3 illustrates the first bending modes for each boundary condition on Abaqus™.

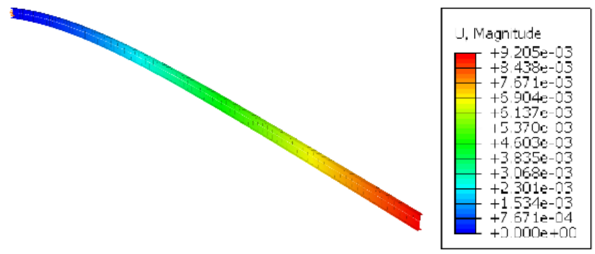

a)

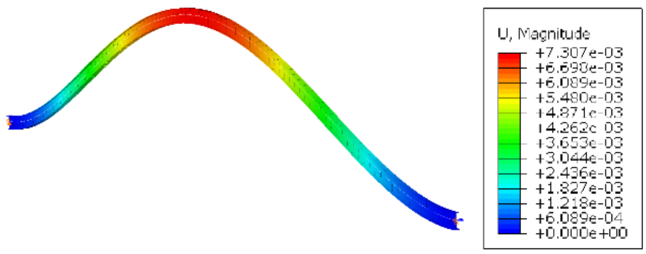

b)

Figure 3 –Mode 1 flexural vibration displacements (not normalised) in mm on FEA beam model for a) cantilever and b) en-castre beam conditions

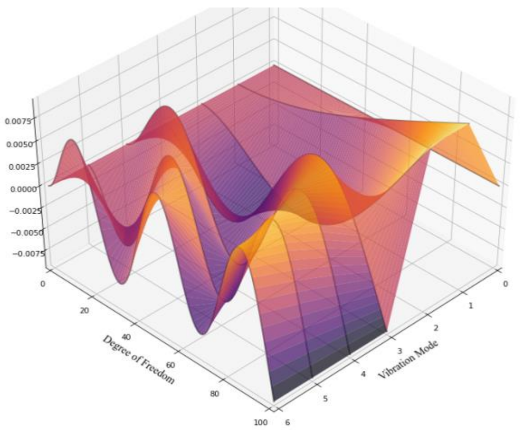

a)

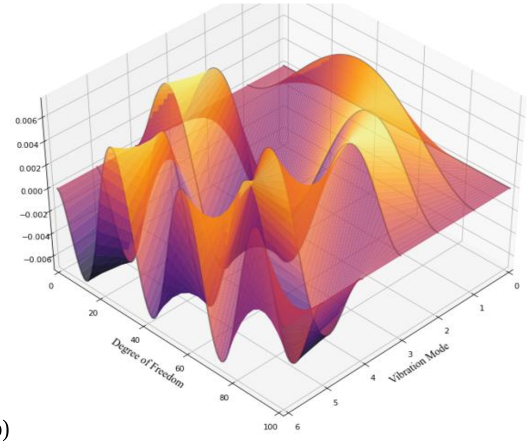

b)

Figure 4 – Modal matrix surface plot of FEA data of both a) cantilever and b) en-castre beam conditions

The surface plot of relative displacements along the first six low-frequency modes for each location is shown in Figure

[28] (ABAQUS, Inc., 2009)

4, used to validate the acquired mode shapes against standard analytical solutions for both beam conditions. This surface was normalised and stored in a modal matrix, $\mathbf{\Phi}$.

A limitation of the model to be noted is the lack of damping. Local damage can influence the natural frequency and modal displacement indirectly by changing the stiffness, mass, and damping ratio of a structure, which should be considered when obtaining information. Generally, damping ratios are difficult to model without introducing non-linear behaviours. A common alternative approach to generating damping information without direct experimental data is proportional damping. However, this was omitted, as damping is an otherwise insensitive parameter to damage. Moreover, the outlined methodology approaches the derivation of the objective functions (as explored in section 3) under assumed system linearity; the Abaqus™ eigenvalue extraction and transient modal analysis procedures are also only applicable in the case of an undamped model due to requiring orthogonality for modal decomposition[28].

3 Objective Functions

An exhaustive amount of literature has been produced regarding SPO within systems. Most early contributions identify optimal positions through the measurement of error sensitivity or regarding the error covariance matrix[29]. Kammer[15] first introduced a method which can be compared to FEA models to directly validate sensor data, by ranking the contribution of candidate sensor locations to the linear independence of corresponding modal partitions. The set of locations is reduced to the number of required sensors by iteration, which allows OAs to be employed.

This paper studies five different applied performance indices derived using the ideology, limited to the assumption that only modal-displacement and natural frequency data were acquired. These strategies include Fisher Information (FIM); Eigenvalue Vector Product (EVP); Effective Independence (EI); Average Driving-Point Residue (ADPR); and a combination of the latter. All methods listed below use the obtained modal matrix, $\mathbf{\Phi}$, and its respective natural frequency array, ω.

3.1 Fisher Information Matrix

Maximising the Fisher Information Matrix (FIM) determinant associated with its parameters to be identified is one of the most widely applied objective function strategies in literature, first proposed by Qureshi[30] as a means of optimising sensor placement in distributed parameter systems. In the context of SHM, sensor information can be viewed statistically as the likelihood of an observable random variable $\mathfrak{R}$ attaining an influencing parameter θ distributed by the function f[31]. The optimum array of sensors can be considered as the underlying distribution, estimated by the random variable of modal displacements, as seen in Equation 3.

$$[\daleth(\theta)]_{i,j} = E\left[\left(\frac{\partial}{\partial\theta_i}\ln f(\mathfrak{R};\theta)\right)^2 |\theta\right] \tag{3}$$

The probability of an observed outcome's information towards a distribution given a known value with regard to the parameter. This is computed as a variance score, known as the FIM. Using spatially independent test modes measured throughout the structure, the best estimation of independent information for a given set of candidate locations can be implied from minimising the covariance matrix of estimate errors[15].

Assuming linear independence, it can be implied for all time such that the output displacements y_i stored in $\mathbf{\Phi}$ can be decomposed into an uncoupled formulation using modal coordinates q and a sensor noise vector $\vec{n}$ in equation 4[32]:

$$y_i = \Phi_i q + \vec{n} \tag{4}$$

The solution which provides an estimate for target states, $\hat{q}$;

$$\hat{q} = [\Phi_i^T \Phi_i]^{-1} \Phi_i^T y_i \tag{5}$$

For a limited set of i sensor locations, a modified form of FI given in Equation 6 enables the covariance matrix of the estimate error $\boldsymbol{P}$ to be computed.

$$\begin{gathered} \boldsymbol{P} = E[(q-\hat{q})(q-\hat{q})^T] - \left[\Phi_i^T (\Psi^2)^{-1} \Phi_i\right]^{-1} \\ \boldsymbol{P}^{-1} = \frac{1}{\Psi^2} \Phi_i^T \Phi_i \end{gathered} \tag{6}$$

For which E is the expected value, which under a random stationary perturbation would be equal to zero, and Ψ is the variance. As the matrix $\boldsymbol{F_o}$ is equal to the inverse of $\boldsymbol{P}$ in the assumption of an unbiased estimate, this expression can be rearranged to

$$\boldsymbol{P}^{-1} = \boldsymbol{F_o} = \sum_{j=1}^{n} [\Phi_{i,j}^T][\Phi_{i,j}] \tag{7}$$

or as the sum of contributions of each candidate sensor location, with $\phi_{i,j}$ as the i-th index of the modal participation for the j^{th} degree of freedom[15]. Note that the variance term is no longer relevant as all sensors are assumed to be identical and thus uncorrelated. By taking the

[29] (S. Omatu, 1978)
[30] (Z. H. Qureshi, 1980)
[31] (E.L. Lehmann, 1998)
[32] (F.E. Udwadia, 1985)

determinant of this matrix, signal intensity and independence can be maximised[33].

3.2 Effective Independence

Effective Independence (EI) is a commonly used objective strategy applied by Kammer and Tinker in an SPO study on the X-33 aircraft[34]. EI aims to seek locations with maximum linear independence contribution to information as quantified by the FIM. By solving the FIM eigenvalue equation using equation 8,

$$[\boldsymbol{F_o} - \lambda \boldsymbol{I_k}]\vec{v} = 0 \tag{8}$$

where λ are the eigenvalues, $\boldsymbol{I}$ is the identity matrix with FIM dimension k, and $\vec{v}$ corresponds to the eigenvectors. It follows that for a set of linear independent sensor sets, $\lambda \in \mathbb{R}^+$ and $\vec{v}$ are orthonormal. By further manipulation, the effective independence coefficient matrix can then be constructed as *E*, where *E* is defined as[35]:

$$E = [\boldsymbol{\Phi}\vec{v}]^2 \lambda^{-1} \Sigma l_k = [\boldsymbol{\Phi}][\boldsymbol{\Phi}^{\mathrm{T}}\boldsymbol{\Phi}]^{-1}[\boldsymbol{\Phi}]^T \tag{9}$$

in which l_k is the array of all coefficients in the k^{th} line. By taking the clinodiagonal entries of *E*, the resulting array entries are notated as $\vec{E}_D$ represents the fraction of the i^{th} sensor towards the full rank of Φ, or the contribution on the corresponding test index on the information matrix. This SPO strategy is iterative and should be performed until the number of target locations is achieved[36].

3.3 Eigenvalue Vector Product

Eigenvalue Vector Product (EVP), also referred to as the Optimum Driving Point (ODP) technique. This method maximises the frequency vibration energy for a given DOF by calculating the product of eigenvector components for all vibration modes of interest. In theory, as the formulation incorporates the factorial operator, Π, candidate DOFS along modal nodes will always lead to an outcome of zero regardless of other contributions[40]. EVP for a specified DOF can be expressed in Equation 10 as:

$$EVP_i = \prod_{j=1}^{n} |\Phi_{ij}| \tag{10}$$

3.4 Average Driving Point Velocity

Developed in the publication by Imamovic and Ewins in 1997[37], ADPV relies on the driving-point analysis within the family of energy-based methods. [38]Driving point analysis relies on comparing the effectiveness of a given sensor location or DOF in its ability to respond at different modes, revealing its vibrational characteristics. The DPV coefficient matrix can be expressed in equation 11 as follows

$$\boldsymbol{DPV} = \boldsymbol{\Phi} \otimes \boldsymbol{\Phi\Lambda} \tag{11}$$

Where $\boldsymbol{\Lambda}$ is the diagonal eigenvalue matrix, operated by element-wise multiplication ⊗. Incorporating the frequency term provides a contribution of each point relative to its global vibration degree. The form equation 12 simplifies a select node's mobility score elementwise, where higher values are indicative of the potential for more significant velocity excitation and, thus, displacement[39]. Lower values, in contrast, show node positions.

$$ADPV_i = \frac{1}{n}\sum_{i=1}^{n}\frac{\Phi_{ij}^2}{\omega_i} \tag{12}$$

$ADPV_i$ assesses the driving point of the i^{th} component within the *ADPV* vector over *n* modes of interest. *i* and *j* denote the i^{th} eigenfrequency and j^{th} element of the i^{th} mode. The *n* denomination acts to average over the modes of interest.

3.5 Effective Independence – Driving Point Velocity

$$\vec{E}_{D_i}^{EIDPV} = \vec{E}_{D_i}^{EI}\, DPV_i \tag{13}$$

Effective Independence can select locations which exhibit low signal strength, leading this strategy to lose information, especially in noisy conditions[39]. By combining the DPV operator with EI, Meo and Zumpano[40] proposed the Effective Independence – Driving Point Velocity method. This allows effective independence to be weighted by an energy indicator[41].

EI-DPV of the i^{th} mode can be calculated in equation 13.

[33] (A. R. Rao, 2014)
[34] (D.C. Kammer, 2004)
[35] (Guimei Gu, 2016)
[36] (W. L. Poston, 1992)
[37] (G. Pasch, 2022)
[38] (Kang Liu, 2018)
[39] (Barthorpe and Worden 2009)
[40] (M. Meo, 2004)
[41] (Y. Tan, 2019)

4 Optimisation Algorithms

Following the selection of applied strategy for SPO as outlined in Section 2, candidate positions can be represented as an optimisation problem in which optimisation algorithms (OAs) can be employed as an alternative to exhaustive search methods. These are procedures used to generate solutions to unknown mathematical processes whilst satisfying provided constraints and parameters. Regarding SPO, the sensor locations correspond to the optimisation variable, constrained by the number of sensors. Many optimisation algorithms exist in the literature and can broadly be categorised into two approaches: deterministic and indeterministic[42]. Deterministic methods generally rely on orders of derivative information[57] retrieved from the objective function at a particular position and encompass linear (LP); non-linear (NLP); and dynamic programming methods (DP).
For the purposes of optimising the modal information of beams, these conventional OA techniques are often insufficient to solve NP-hard SPO problems - as both the objective function and constraints are continuous and multivariate in nature. Due to the deterministic nature of the search, traditional techniques are limited and may not guarantee that global solutions will be found, especially as dimensionality increases[43]. In the last two decades, higher-level meta-heuristic OAs such as "memetic" algorithms[44] and the use of neural networks have been employed[45]. This paper studied several of the former and attempted to program their standard forms using Python to ensure ease of implementation in practice and controlled comparison. Any variations made to the algorithm have been justified as trivial to modify.

Early memetic algorithms were developed in the 1970s to overcome the limitations of conventional methods[46]. These are referred to as such due to their analogy to biological phenomena which incur change[47]. The solutions of memetic algorithms are meta-heuristic and stochastic, defined by their inherent randomness and probabilistic transition rules independent of the objective, possessing a perceptible learning mechanism. This statistical approach is advantageous to modelling uncertain outcomes subject to complex or dynamic variables. These OAs can be broadly characterised into two categories: Evolutionary (EA) and Swarm Intelligence (SIA) algorithms. A multitude of such algorithms exists, including Ant Colony Optimisation (ABO), Bacterial Foraging Optimisation (BOA), and Cuckoo Search (CS), all simulating different aspects of biological processes[48]. For the purposes of this paper, three classes of the most common memetic OAs in literature were compared: Genetic Algorithm, Differential Evolution, and Particle-Swarm Optimisation.

As these methodologies are meta-heuristic, optimal solution search and performance are often solely dependent on an adequate selection of internal variables which govern each respective computation, known as hyperparameters. This is often a challenging and recurring subject of debate throughout the investigation; their values directly impact the outcomes of each OA alongside convergence but are highly dimensionally dependent. In general, most parameters act stochastically in the form of probabilistic thresholds. Such parameters, when increased, will tend to lead to faster solutions through reduced random search and retaining quality solutions but may cause premature local optima settling or overshooting if not disrupted. A balance must be struck between local and global explorative diversity. Any hyperparameters chosen have been justified through existing literature.

4.1 Genetic Algorithm

First proposed in 1975[49], Genetic Algorithms (GA) are the most applied class of evolutionary algorithms, using a simulation involving operators analogous to the mechanisms of Darwin's theory of evolution. Through selective adaptation within a competitive environment, a set of individuals possessing a higher "fitness" are more likely to survive. GA presumes an individual, formulated by a series of concatenated alleles, to be a candidate for the problem, represented by a set of parameters. The quantification of fitness can be evaluated through minimisation or maximisation of the objective function. Each subsequent generation is created by stochastically selecting a small group of individuals to reproduce the next generation, and this cyclical operation is repeated until a termination criterion is reached[50]. Fundamentally, GA applies operators including, in respective order [51]:

- Encoding: Parameterizing the problem inputs and constraints into an individual by encoding information into a structure known as a bitstring, analogous to a genome.
- Selection: A schema used to evaluate and determine the individuals based on their fitness and methodically select parents for the next generation.

[42] (P. Gao, 2021)
[43] (I. Ahmandianfar, 2017)
[44] (Vijendra Kumar, 2022)
[45] (T. Marawala, 2006)
[46] (R.V. Rao H. K., 2018)
[47] (X. Yu, 2010)
[48] (Wei Li, 2021)
[49] (John, 1975)
[50] (K.F. Man, 1996)
[51] (B. Alhijawi, 2023)

- Crossover: Function operating on a select pair of parents in a similar form to mating, where each genome is recombined to produce new solutions.
- Mutation: Random deformation of an individual under a specific probability to introduce new solutions.

Due to its independence from the objective function, many techniques have advanced across the literature, introducing variations for each operation[52]. The variant of GA herewith used in this paper employs integer-encoding/Roulette fitness proportionate and k elitism selection/Single-point crossover/Single-point mutation operation techniques. This form is presented in Algorithm 1.

Algorithm 1: *k*-Elitist Genetic Algorithm

$t = 0$
Initialise random population P^t of size *N*
while `StoppingCriterion` not reached **or** *t* < `maxGen`:
  Evaluate fitness for individuals $f(P_i^t)$
  Select *k* `EliteParents` using $R^{t+1} = \max[f(P_i^t)]$
  Select $\frac{N-k}{2}$ `NormalParents` using Roulette Selection with probability $\mathbb{P}_{s,i}$
  Perform crossover for pairs of `NormalParents` with probability $\mathbb{P}_{c,i}$ to produce Q^{t+1}
  Mutation operation for individuals in Q^{t+1} at rate $\mathbb{P}_{m,i}$
  Form new generation of parents $P^{t+1} = [R^{t+1}, Q^{t+1}]$
  Compute $f(P_i^{t+1})$
  $t += 1$
end while

Integer encoding refers to the process in which information is stored within individuals *i* as a serial bitstring of integers of size *D*, where *D* represents the number of solution modes – i.e. the number of candidate sensors in discretised locations belonging to $\{\vec{x} \in \mathbb{Z}^+ \,|1 \leq \vec{x} \leq N\}$. Despite binary encoding being more prevalent across literature and ease of implementation[50], it is unable to guarantee that a genome solution set equals *D* for all mutated individuals when performing bitwise replacement. Hence for any iteration *t*, the population, P^t can be designated as:

$$P^t = \begin{bmatrix} \vec{x}_1^t \\ \vec{x}_2^t \\ \vdots \\ \vec{x}_N^t \end{bmatrix} = \begin{bmatrix} x_{1,1}^t & x_{1,2}^t & \dots & x_{1,D}^t \\ x_{2,1}^t & x_{2,2}^t & \dots & x_{2,D}^t \\ \vdots & \vdots & \ddots & \vdots \\ x_{N,1}^t & x_{N,2}^t & \dots & x_{N,D}^t \end{bmatrix} \quad (14)$$

Multiple methods of selection were considered to direct the general population fitness of GA across iterations by evaluating the objective function, generalised into either fitness proportionate or ordinal selection[53]. Roulette-selection is an example of the former, directly assessing an individual's probability for selection directly as a function of its individual fitness value as described in Equation 15[66].

$$\mathbb{P}_{s,i}^{t+1} = \frac{f_i^t}{\sum_{j=1}^{N} f_j^t} \quad (15)$$

where $\mathbb{P}_{s,i}$ is the probability for an individual i to be selected by computing the degree of fitness f. *k*-Elitism retains *k* number of individuals with the highest fitness to be carried over into the new population set that is exempt from crossover and mutation operations to ensure the best solutions are carried forward.

In a one-dimensional solution space, the stochastic nature of mutation and crossover operators is limited, and any degree of complexity was considered excessive when introduced at the cost of convergence. Thus, only the simplest forms of both were used. Single-point crossover operates between a pair of parents by exchanging tail genes past a random crossover point within the parental genome to produce a pair of higher-quality offspring at a certain probability $\mathbb{P}_{c,i}$ = 0.1,[26];

The crossover vectors Q_i^{t+1}, Q_j^{t+1} are produced in the following generation. These set of solutions are then passed into the single-point mutation operator, acting to select a random gene within the offspring for a different non-repeating integer with a probability dictated by a mutation rate ranging from $\mathbb{P}_{m,i} \subset [0,1)$. Though optimal mutation probability is dependent on the size of the population, probabilities for integer-encoded GAs should be higher than binary-coded GAs[54]. For $\mathbb{P}_{m,i}$, a static limit can be approximated using $m = \frac{1}{D}$[55]. The result is appended to the existing set of elites and set as the population for the successive generation.

[52] (S. Katoch, 2020)
[53] (Sastry K, 2014)
[54] (Wright, 1991)
[55] (R.N. Greenwell, 1995)

4.2 Differential Evolution

As the second most popularly applied class of Evolutionary OA within SHM, Differential Evolution (DE)[56] can be applied to solve optimisation problems globally through iterative metaheuristic search. Like GA, DE algorithms are derived from the Theory of Evolution, using similar mutation, crossover, and selection operators. The main differences of DE are: DE lacks an encoding strategy, instead operating directly on candidate solutions defined as real vectors on an optimisation domain size *D*; characteristic mutation strategy and gradual individual replacement in favour of generational replacement through calculating the difference of parameter vector pairs.

The paper investigates a form of DE as recommended by Ortiz and Xiong in 2014, notated as DE/current-to-best/1[57]. Current-to-best notates the vector selection strategy in mutation, and 1 denotes the number of difference vectors employed in the weighted difference calculation[58]. Initial formulations of DE algorithms often use DE/rand/1 as a foundation point for improvement. However, DE/current-to-best/1 was recommended for best performance and accuracy regarding multi-modal optimisation problems[59].

A mathematical model for the DE paradigm applied begins with the initialisation of a maintained population with size *N* as a set of individual candidate vectors as $\vec{x}_i^t = \langle x_1^t, x_2^t, \dots, x_D^t \rangle \in \mathbb{R}^D$. Unlike GA, the stochastic operators are introduced first. For all individuals, *i*, a mutation operator acts to select two unique individuals from the current iteration and performs a weighted difference scaled by a mutation factor $F_1, F_2 \in [0\,,2]$ to facilitate randomness.

$$v_i^{t+1} = x_i^t + F_1\left(x_{best}^t - x_i^t\right) + F_2\left(x_{r1}^t - x_{r2}^t\right) \qquad (16)$$

The resulting vector v_i^{t+1}, as calculated in the formula above, is produced by random selection of target vector individuals in the current generation x_{r1}^t, x_{r2}^t scaled into a weighted difference using the current best individual within the generation x_{best}^t . Each enumeration of the mutation vector set enters crossover, which acts to accept this solution as a trial solution vector based on a given crossover probability $CR \in [0\,,1]$., or as encoded in Equation 17

$$u_i^{t+1} = \begin{cases} v_i^{t+1} & \text{if } j \le CR \text{ or } i = I_r \\ x_i^t & \text{otherwise} \end{cases} \qquad (17)$$

such that $j = \text{rand}\{x \in \mathbb{R}^+ \mid 0 \le x \le 1\}$, and $I_r = \text{rand}\{x \in \mathbb{Z}^+ \mid 1 \le x \le N\}$. Crossover ensures increased diversity of the perturbed parameter vectors, leading to a set of trial vectors u^{t+1}. Clamping was implemented to ensure elements of the set were appropriate by ignoring any solutions generated outside of the bounds of the problem.

$$x_i^{t+1} = \begin{cases} u_i^{t+1} & \text{if } f\left(u_i^{t+1}\right) \ge f(x_i^t) \\ x_i^t & \text{otherwise} \end{cases} \qquad (18)$$

Equation 18 formulates the roles of the selection operand, where f is the fitness function used; creating the list of the succeeding generation x^{t+1} . As with GA, this process is repeated until a termination criterion is reached. Due to a smaller set of hyper-parameters to optimise, DE is typically cited to be more robust and have faster convergence[59]. Its absence of an encoding scheme is also advantageous to solving non-linear and non-differentiable functions. From Wang et al.'s current-to-best scheme, the choice of *F* = 0.8 and *CR* = 0.2 was used[60]. A code model of the DE algorithm used in this study is provided below:

Algorithm 2: DE/current-to-best/1 Differential Evolution

```
t = 0
Initialise random population P^t of size N
while StoppingCriterion not reached or t < maxGen:
    for i in P^t:
        Select x_r1, x_r2 unique TargetVectors at random
        Calculate MutantVector from weighted difference
        Generate random numbers j and I_r
        if j ≤ CRrate or i = I_r:
            TrialVector ← MutantVector
        if f(TrialVector) ≥ f(P_i^t):
            P_i^t ← TrialVector
    end for
    t += 1
end while
```

[56] (R. Storn, 1996)
[57] (M. Leon, 2014)
[58] (W. Gong, 2013)
[59] (M. Georgioudakis, 2020)
[60] (Y. Wang, 2021)

4.3 Particle Swarm Optimisation

Unlike the previous OAs, Particle Swarm Optimisation (PSO) is not classed as an evolutionary algorithm but instead based on swarm intelligence, finding solutions through mimicking social behaviours exhibited by the navigation and coordination of swarm-based animals through emergent complexity. First introduced in 1995,[61] The PSO search strategy involves candidate solutions treated as individual particles, dispersed over a *D*-dimensional search space optimisation space, for which successive iterations update the direction of movement influenced by the combination of personal and social components. Likewise, to GA, PSO literature is extensive and has facilitated many modifications over recent decades; the form of PSO employed in this study was modified based on the studied literature and feasibility. *N* particles are initialised at random or using a distribution, as presented. The collective positional argument vector of the population for any iteration *t*, can be expressed as $\overrightarrow{X^t} = \langle \overrightarrow{x_1^t}, \overrightarrow{x_2^t}, \dots, \overrightarrow{x_N^t} \rangle$ such that each particle is formulated by $\overrightarrow{x_i}^t = \langle x_{i,1}^t, x_{i,2}^t, \dots, x_{i,D}^t \rangle \in \mathbb{R}^D$. For each sequential generation *t*+1, a velocity vector $\vec{v_i}^{t+1}$ is assigned for each particle, imparting an initial direction and intensity of movement. This velocity vector is procedurally generated using Equation 19, defined by the vector sum of inertial, cognitive, and social components, respectively, to update the particles' positions towards the solutions.

$$v_{ij}^{t+1} = w^t v_{ij}^t + \kappa_1 r_1 \left(p_{best,ij}^t - x_{ij}^t\right) + \kappa_2 r_2 \left(g_{best,j}^t - x_{ij}^t\right) \tag{19}$$

$$w^{t+1} = w^t + 0.5e^{-|p_i^t - p_{i,best}^t|} \tag{20}$$

- Inertial: *w* component to maintain the current velocity of the particle from the previous iteration, for which its resolution can be dynamically decreased over generations. It is common practice for search OAs to gradually permute from exploration to local exploitation across generations to improve refined searching around solution seeds. Typical ranges of $w \in \mathbb{R}^+$ will range from [0.9, 1.2]. Though linear proportional decrease is a common method[62], this paper opted to implement an exponential relationship, which is evaluated independently for each particle within an iteration to adapt to situational capabilities[63].
- Cognitive: Described as the difference of a particle's best position found $p_{best,ij}^t$ cumulatively across all prior generations, and its current position
- Social: Direction component towards the generation's best solution $g_{best,j}^t$ across generations thus far, defining an attractor for the cumulative swarm.

κ_1, κ_2 are static acceleration coefficients set to dictate the scale of influence of each component between the explorative and exploitative aspects derived from the personal and global parameters, respectively. According to optimal static values following $\kappa_1 + \kappa_2 > 4$ [64], and the understanding that multi-modal problems tend to prefer a bias towards a more considerable cognitive contribution, $\kappa_1 = 2, \kappa_2 = 2.2$ were used. Inherent stochasticity was introduced using $r_1, r_2 = \text{rand}\{r \in \mathbb{R}^+ | \ 1 \le r \le 2\}$.

$$x_{ij}^{t+1} = x_{ij}^t + v_{ij}^{t+1} \tag{22}$$

This velocity vector is then subtended for all position vectors to calculate a new trajectory for the next generation. The fitness function is then calculated for all current particles, after which the iteration process is repeated until sufficient convergence is exhibited or the maximum number of iterations is reached, as illustrated in Algorithm 3:

Algorithm 3: Particle Swarm Optimisation Algorithm

```
t = 0
Initialise random population P^t of size N
while StoppingCriterion not reached or t < maxGen:
    for i,j in P^t:
        Generate random numbers r_1 and r_2
        Calculate velocityVector
        positionVector ← positionVector + velocityVector
        if f(positionVector) ≥ PersonalBest
            PersonalBest ← positionVector
    end for
    if f(all(positionVector)) ≥ GlobalBest
            GlobalBest ← TrialVector
    Update w
    t += 1
end while
```

[61] (R. Eberhart, 1995)
[62] (Y. Shi, 1998)
[63] (P. Chauhan, 2013)
[64] (Clerc, 2002)

4.4 Optimisation Hyperparameters

No statistically significant difference between optimum solutions arises from tuning stochastic parameters of each OA, as such standard values from the literature were implemented. In contrast, altering the population size is the external parameter with the most effect on performance across literature[65], with most articles stating selection is dependent on the search space's smoothness and its dimensionality. As dimensionality increases, the probability of solutions covering favourable regions decreases for a given population. In contrast, a larger population will be more computationally intensive[51]. A GA study conducted on E. coli in 2013 concluded a minimum population of 20 was required to achieve a better solution, with 100 chromosomes being optimal under similar parameters[66]. PSO and DE algorithm population sizes can be smaller without the deterioration of performance; due to the individualistic mutation process, performance can remain high, which lends itself to an advantage[67]. Empirical studies show that a population size of 30-50 is sufficient for most DE problems, and a population of 10-30 is sufficient for most PSO problems of this scale[59,68]. The table below outlines the different populations used within each OA.

OA	GA	PSO	DE
Population Size	100	20	50

Another major challenge of implementing OAs is defining an appropriate termination criterion to end the search process when the algorithm degenerates, or no significant improvement can be expected within a reasonable number of iterations. A variety of such criteria exist in literature, classified into three main categories: direct, derived, and cluster-based[69]. Early OAs implemented direct termination, ending the algorithm when a predefined condition is met without considering underlying data. As these are the most straightforward classes to implement, this was used for further studies[70]. For consistency, the stopping criteria for all OAs used a combination of i) T maximum generation threshold and ii) K-iteration convergence criterion. The former stops the OA once the maximum allowable number of iterations is fulfilled, while the latter defines the best fitness variance sustained over K generations. Intuitively, as both $T, K \to \infty$, the probability of reaching an optimal solution tends to 1. As the values of T and K are chosen arbitrarily based on the bitstring length, a generational limit of T = 10,000 was chosen, with a 99.9% best fitness similarity for a set preceding $K = 15$[71].

5 Results

5.1 Optimal Sensor Layout

The optimal sensor layouts for each respective OA and Objective Function under both boundary conditions are displayed in Figures 5, 6 and 7. Each converged sensor location is marked in a red cross. As global search OAs are stochastic in nature, an average of 50 tests were run to establish a statistical distribution of the solution with a good statistical confidence level.

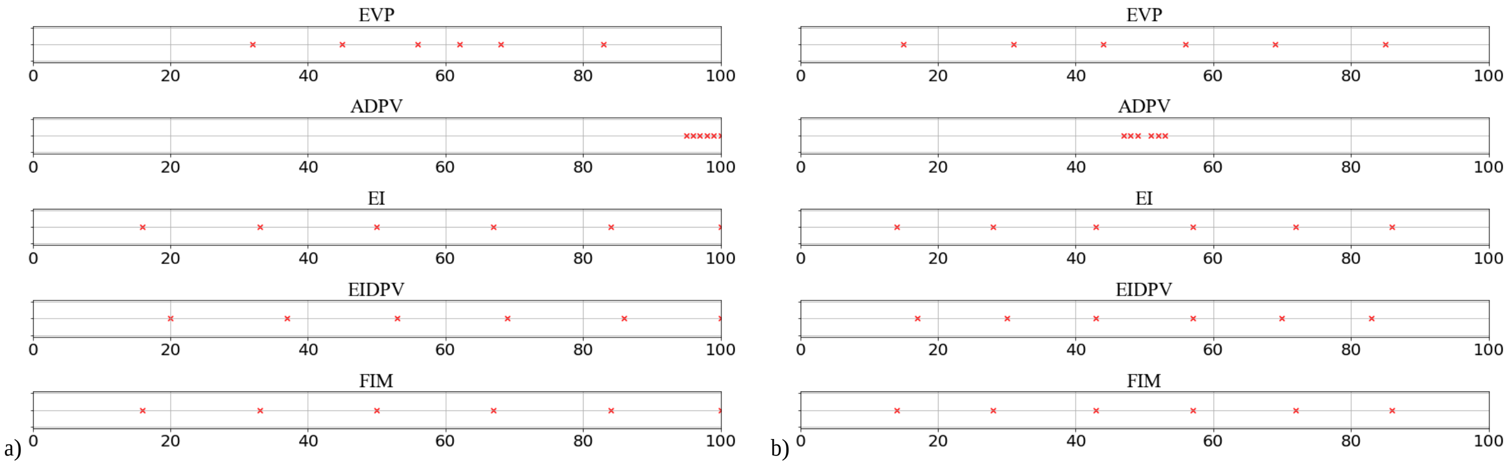

Figure 5 – Differential Evolution a) Cantilever and b) En-castre OSL

[65] (A. Alajmi, 2014)
[66] (O. Roeva, 2013)
[67] (B. Bhattacharyya, 2007)
[68] (Qatar)
[69] (B. Jain, 2001)
[70] (S. Ghoreishi, 2017)
[71] (D. Bhandari, 2012)

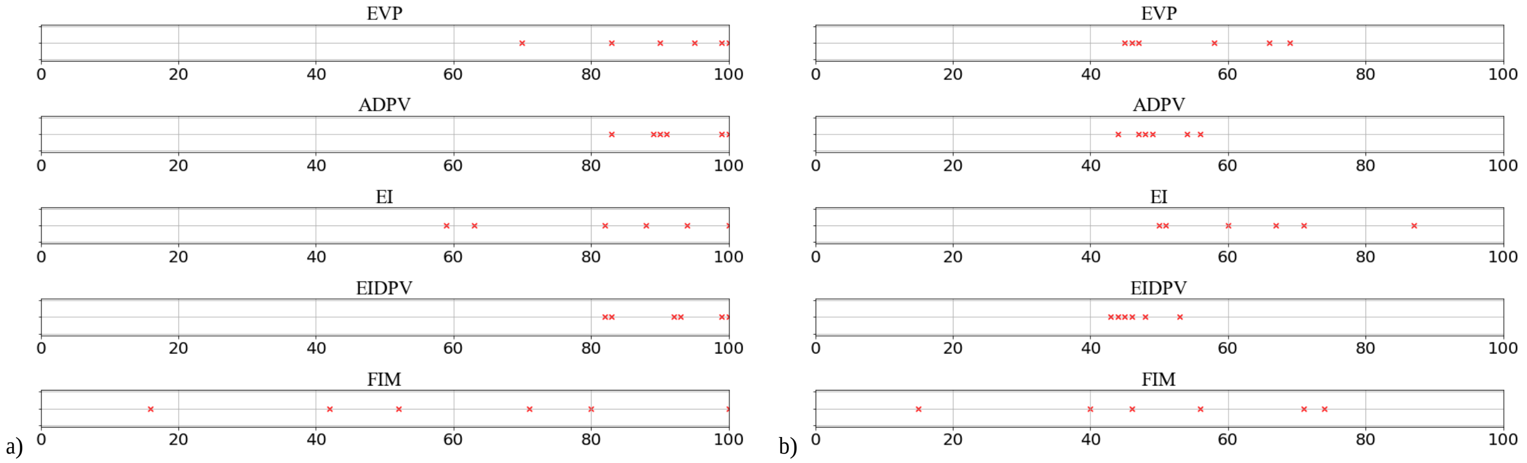

Figure 6 – Genetic Algorithm a) Cantilever and b) En-castre OSL

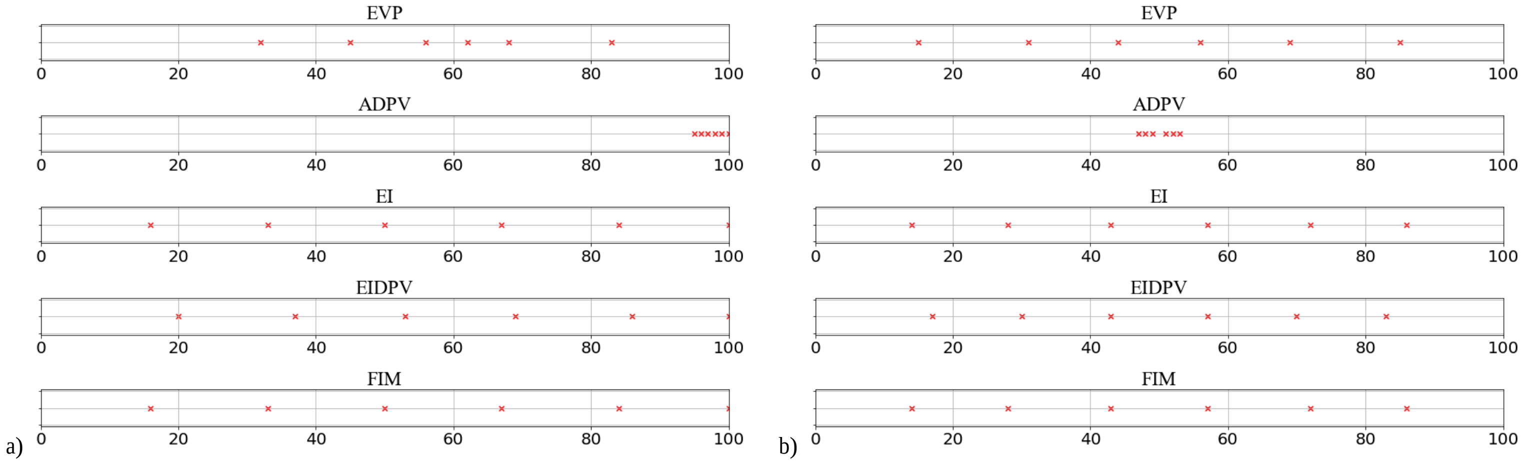

Figure 7 – Particle Swarm Optimisation a) Cantilever and b) En-castre OSL

From Figures 5 and 7, it can be shown that PSO and DE algorithms converge to identical OSL for each given objective function. This contrasts with GA whilst observing and conducting multiple simulations, where convergence solutions are inconsistent at best. Several studies reviewed have mathematically proven that GA converges to a global optimum and, in cases of convergence, is only to a degree of precision[71,72]. The apparent discrepancy in GA's performance is likely due to the suboptimal nature of optimisation in the context of a single-dimensional solution space with multimodality. GA attempts to generate entirely new population sets through recombination for each iteration of the population, which risks disrupting converging solutions as they get replaced. A similar issue arises from how the objective function is evaluated for a whole set of solutions within a single individual, as opposed to considering each allele. This can lead to a variance in unique layouts reaching an identical or similar fitness level. Despite elitism, the number of best solutions could not be retained without premature convergence occurring. Based on these factors, the intrinsic stochasticity of GA is much higher than that of both DE and PSO. Though this may lead to the conclusion that GA is ineffective in this case, the OA is proven to be viable for more complex engineering problems with higher dimensionality. In these situations, it is often appropriate as absolute preciseness is not required due to the uncertainty of initial parameters[72].

When further analysing the differences between the results of each objective function, EI, EVP, and FIM converge to similar results, particularly under bounded beam conditions. The EI and FIM methods evaluate identical solutions when comparing DE and PSO algorithms; this is due to how the information matrix is derived directly using the Fisher Matrix; with higher cardinality, Effective Independence has been shown to yield varying configurations[72]. FIM also appears to bear the most similarities across all OAs, suggesting its respective information function contains prominent and distant local minima, which can be converged reliably.

A notable case can be observed by the results using the ADPV criterion across all OAs, in which an OSL experiences sensor clustering. When reviewing the formulation, the ADPV for each candidate sensor location

[72] (G. Ferreira Gomes, 2018)

places the natural frequency term, ω_i, in the denominator which decreases the relative contribution of higher frequency modes as a means of correcting for noise. As these intermediate amplitudes are prevalent only in higher modes, such locations are less likely to be evaluated as viable solutions by this criterion. The influence of ADPV towards EI-DPV is discernible as its layout shows a combination of EI values exhibiting a translation in a direction towards areas of high information in low modes, i.e. where sensor clustering occurs. The degree of translation appears to be systematic, ranging between 2-3 integer values in the fixed configuration and 3-4 values in the cantilever when analysing OSL retrieved from DE and PSO. In GA, EI-DPV indicates a larger contribution from the ADPV components, with evidence of sensor clustering in similar regions.

Finally, when discussing the OSL obtained by the EVP criterion, the bounded case has more similarities with the results obtained by EI, FIM, and EI-DPV. In contrast, the cantilever OSL appeared to be asymmetrical and unevenly spaced. As with EI-DPV, the GA case also appears to display some signs of sensor clustering. This recurring tendency of GA possibly indicates a lower sensitivity to local extrema.

OSL within cantilever conditions generally favour an asymmetrical distribution towards the free end, with most objective functions positioning at least one sensor at the 100th node. In the restrained case, OSL is generally symmetrical from DE/PSO results, closely following the trend in the mode shape. It can be observed that, for most functions, optimal locations are found near locations experiencing high vibration amplitudes, which correlate to regions of high modal information. This behaviour is evident in the cantilever condition, where the unconstrained end experiences more significant deflection and thus contributed to a greater measure of information. Other optimum points are found by accounting for the anti-node positions in higher modes. In bounded conditions, the distribution is more symmetrical, with the exception of GA, which can be attributed to general inconsistencies. Despite the layout heavily corresponding to the vibration amplitudes, due to the nature of multiple modes, OSL is not necessarily trivial.

5.2 Algorithm Convergence

The figures – 8, 9, and 10 – show convergence of values normalised and plotted on a logarithmic scale over the number of iterations for each objective function. For each iteration, a plot was drawn for the "best" and "average" values, notated in solid and dotted lines, respectively. The individual within the iteration resolving to the highest fitness value forms the "best" fitness position, whilst the "average" accounts for all individuals within the population.

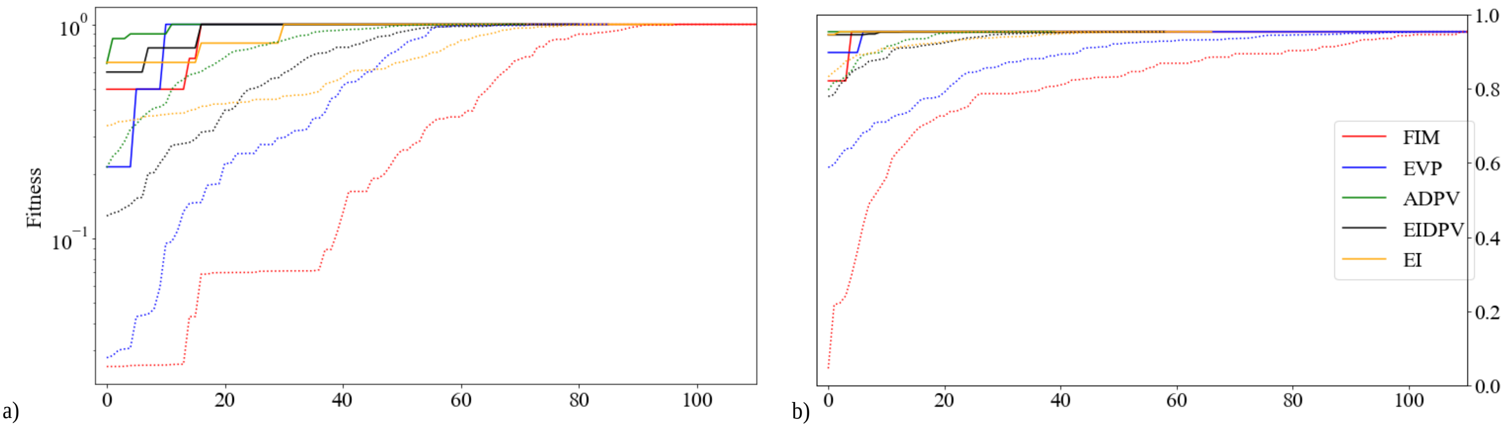

Figure 8 – Differential Evolution a) Cantilever and b) En-castre convergence plot

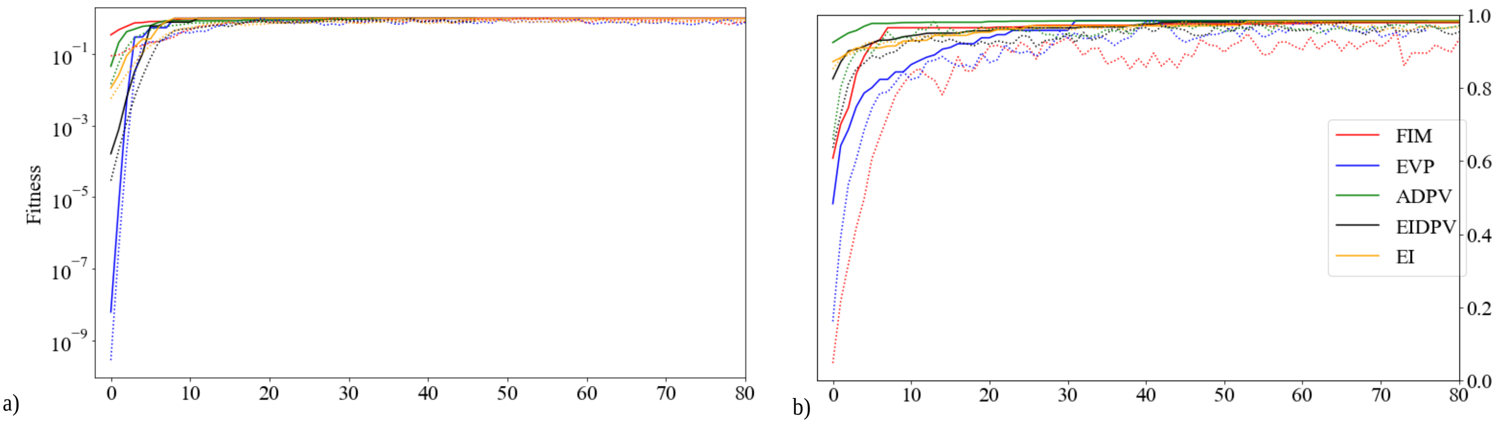

Figure 9 – Genetic Algorithm a) Cantilever and b) En-castre convergence plot

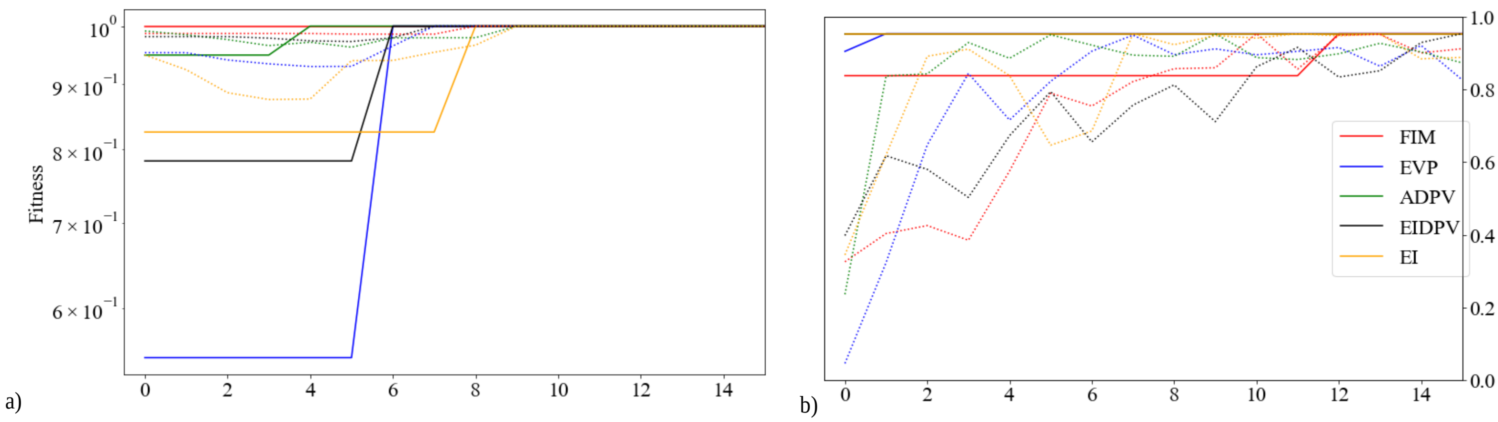

Figure 10 – Particle Swarm Optimisation a) Cantilever and b) En-castre convergence plot

Across all OAs, GA shows the most rapid rate of convergence with respect to the population size, followed by PSO and DE, with convergence to within 1.72x10^{-7}% of the maximum value within >10 generations. The large variance in initial fitness is likely due to the significantly more extensive solution space. For the given problem, there exists D^n possible sensor configurations, as opposed to nD configurations in DE and PSO. DE exhibits similar convergence patterns, though in a much smaller solution space, especially when observing the FIM methodology. This implies that assuming consistent scaling, GA is likely to outperform DE for more complex optimisation situations with more extensive solution spaces. However, it should be mentioned that although initial convergence is rapid, GA appears to find difficulties in converging past a certain level of accuracy, as the stopping criterion was not satisfied until a much larger number of iterations was reached – possibly attributed to GA's entire population replacement as outlined previously. Other studies also recognise GA's inability to guarantee the global optimum is found, coining the term "Genetic Drift"[73].

The advantage of DE in this study lies in the convergence when comparing cantilever and fixed beam boundary conditions, in which DE is the only OA to show faster convergence in the latter case. As shown in Figure 9b and Figure 10b, average values in en-castre beam conditions tend to stabilise toward the optimum much more slowly and experience oscillatory behaviour with a greater stabilised variance. Such a response, which is prevalent in GA, can indicate premature convergence at local extrema. This does not appear to happen in the case of DE, leading to the study concluding that DE is more robust [74] when searching for multimodal solutions within small dimensionalities.

Comparatively, in PSO, convergence occurs rapidly within the least number of iterations, which holds for most produced articles[63]. However, it is important to consider in the context of a small one-dimensional search space that the stochasticity of initial population positions can evaluate the optimal location within the starting generation, which can be observed in some objective functions where no "best" improvement happens. This is especially apparent in Figure 10b. A large population relative to the available solution domain introduces more noticeable discrepancies while evaluating the fitness function between each simulation. This causes the convergence of PSO to be more reliant on the initialisation of individuals. A similar phenomenon was also observed to some degree while employing DE, as both algorithms pertain to similarities in how individuals are generated[74], albeit the variance between convergence rates is much more consistent over repeated executions.

5.3 Noise Resilience

Noise resilience is a pertinent metric for a successful SHM system, defining its robustness to ambient loading conditions; measurement noise from sensors; and environmental contributions[23].

Random noise was introduced to assess the resilience of each objective function when external factors cause disruption to typical data acquisition. To attain the most reliable results, DE was the employed OA from earlier demonstrations of robustness and solution consistency for all experimentation in this section. Gaussian Noise is the standard approach used to introduce random perturbations into the sensor data[75]. A noise signal was generated with a normally distributed probability density function superimposed onto the original modal data.

For the experiment, 3% and 2% of modal and natural frequency noise standard deviations were added onto their respective signals[77]. A set of 20 trials was run using DE, with the resulting OSL frequency distributions represented on a histogram in Figure 11. OSL in noiseless conditions are also plotted to illustrate the correspondence between optimal values and the impacts of noise.

[73] (Booker, 1987)
[74] (J. Vesterstrøm, 2004)
[75] (Boashash, 2016)

Assuming noise does not influence the resulting information function, it can be expected for *n* trials; each extremum would be found with a frequency of *n*. This can be illustrated in the figure labelled EVP control. With the introduction of noise, uncertainty is introduced to the convergence locations, causing convergence in suboptimal positions. An additional calculation was done to determine the average number of sensors found for each objective function used by dividing the total frequency by the number of trials. Unlike the control, the presence of noise introduces small local optima to which additional candidate locations prematurely converged, indicating a significant modification to the information function, such as additional weak local optima with respect to its neighbourhood structure[76].

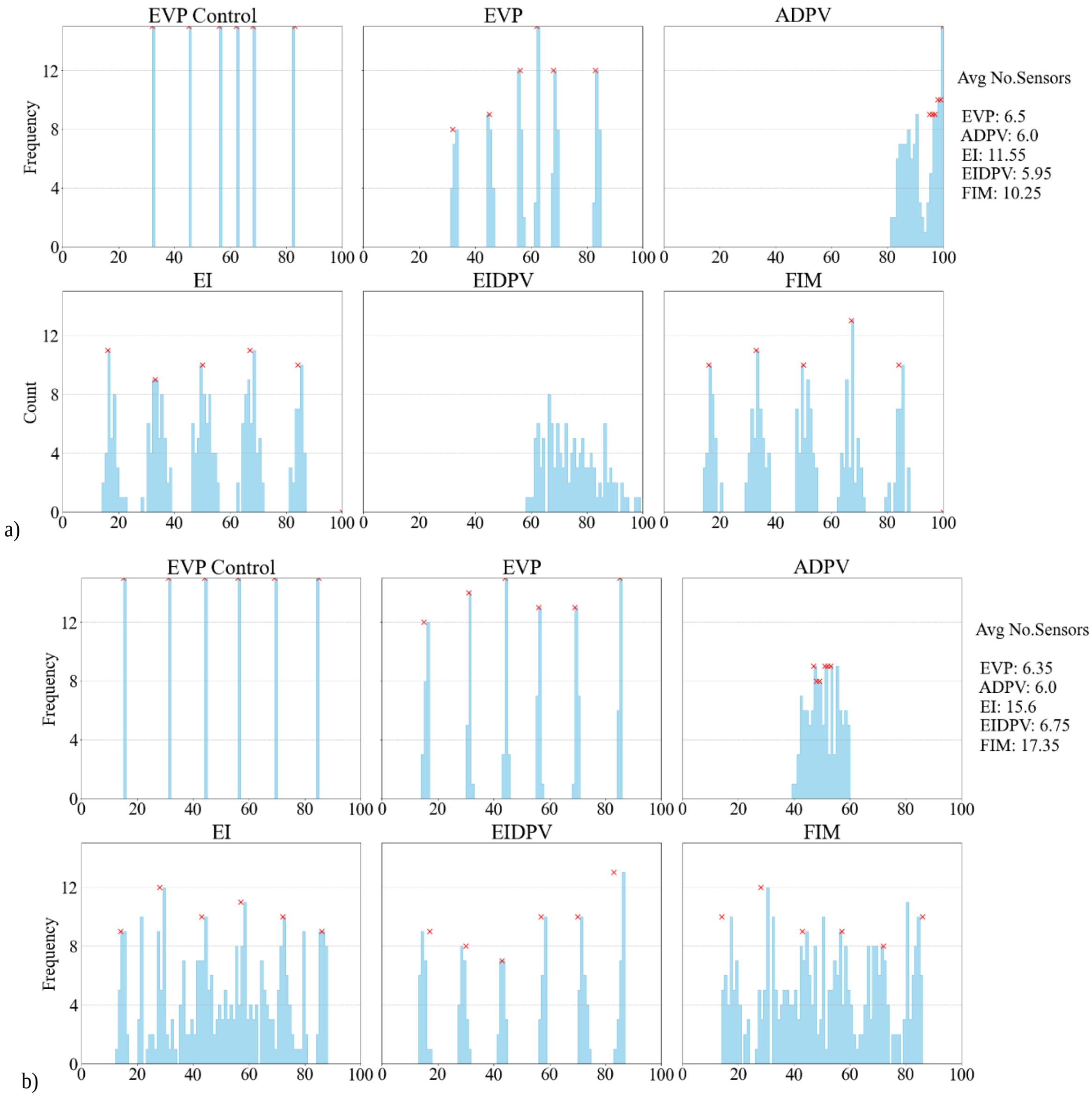

Figure 11 – Frequency plot of OSL locations with introduced noise in a) Cantilever and b) En-castre beam

From the average number of sensors located in the presence of noise, in both cases, both FIM and EI locate a significant number of local optima, averaging above ten SPO results for a single trial in both beam conditions, indicating a vulnerability to such form of noise. The effect of noise was also noted to be higher for these functions in the bounded beam configuration than the cantilever. When examining the distribution, the density of EI and FIM shows a more considerable variance, which may be a consequence of less distance between original OSL peak values. This phenomenon is supported by the paper discussed by Barthorpe and Worden[39], as outlined in section 3.5.

Both EVP and ADPV are criteria which appear least influenced by environmental noise. In particular, the OSL of EVP is in the best agreement across both beam conditions, noise and noiseless conditions. This resilience of its information function can plausibly be explained in EVP evaluating the product of its constituent modes. In contrast with other metrics which evaluate the sum, an eigenvector element contributing vibration energy information will have its effects multiplied, leading to more prominent maxima.

[76] (Baudin, 2011)

EVP is also especially advantageous when avoiding nodes, as these positions will evaluate to zero regardless of noise, attributing to its lack of sensor variance.

Examining the ADPV criterion, the average number of candidate locations equals the expected number of locations across 20 trials. However, this does not indicate a sensor arrangement unaffected by noise, as there is evidence of some distribution around the sensor clusters. From this and the evidence of sensor clustering in OSL, the study concluded that ADPV pronounces the information in the lower modes to an extent unaffected by the inclusion of noise. The positive effect of ADPV on noise resilience[40] is noticeable when observing the EI-DPV method, where the number of sensors located is significantly reduced after weighing the EI algorithm values. This lowered uncertainty in EI-DPV is beneficial, especially in the en-castre beam; however, it appears to fail to converge accurately to the original optimums of degrees 20, 33, and 50 – approaching a distribution closer to ADPV. Thus, EI-DPV was deemed an unsuitable methodology in the context of a cantilever beam.

6 Discussion

6.1 Conclusion

From applying the matrix objective criteria and optimisation under the evolutionary algorithms, the performance of each pair was assessed. The results show that DE and PSO are most consistent in this problem with single dimensionality. Between PSO and DE, DE shows the most consistent convergence rates; considering the average population fitness, it is observed that despite rapid convergence, the variance across multiple executions is more prevalent in PSO from the effects of initialisation randomness. This is consistent with the findings by Vesterstrøm[74], for which PSO and DE outperform GA in problems of low dimensionality. When generalised to a higher number of modes to search, this may lead to a tendency for premature convergence.

The major advantage of GA within the study is the ability to perform multi-modal optimisation without requiring multiple iterations to find all candidate solutions for a single generation. However, GA uses a lot of hyper-parameters that require prior settings, increasing its difficulty in implementation. Despite DE and PSO reaching a more deterministic solution over successive iterations, the problem is only one-dimensional, with a low number of modes of interest. Although DE/PSO are objectively more reliable, small problems may favour conventional exhaustive search. As both complexity and dimensionality increase, GA is shown to outperform both algorithms.

While DE is established as the best performing OA, the best objective function remains dependent on the specific boundary condition. As mentioned, the resulting sensor layout of EI, FIM, and EI-DPV share many similarities, which can lead to confidence in the OSL when using the following metrics. All metrics find optima in close proximity to regions of high amplitudes. ADPV is the exception, as the function is prone to sensor clustering and, thus, should be avoided as an independent measure. With regards to EVP, the conclusion is case-dependent: with the bounded boundary condition, the similarities are evident; however, in the cantilever, this is not as apparent. In section 5.3, noise resilience was investigated. Within both cases, EVP shows the highest resilience to environmental noise, with FIM and EI both being the most vulnerable. By combining the fractional contribution provided by ADPV with EI, the resulting uncertainty in EI-DPV was mitigated to an extent, particularly in the en-castre configuration.

From these observations, this study identifies EVP/DE as the best strategy for SPO within a cantilever beam and EI-DPV/DE as the best strategy in the fixed beam, with the proposed layouts as positions [32,45, 56, 62, 68, 83] and [17, 30, 43, 57, 70, 83] respectively.

6.2 Validation

Without proper experimentation using fatigue loading, it is difficult to ascertain the validity of an OSL with confidence; regardless, an alternative was achieved using FEA. From section 1, it is noted that damage is typically related to changes representable by an elemental stiffness reduction factor[26]. Validation was performed on the cantilever beam using a methodology outlined by S.K. Panigrahi, in which experimental data within a damaged beam was artificially modelled in Abaqus™ through stiffness reduction of a set number of elements[6,77]. To closely imitate the conditions in the specified study, the Young's Modulus of elements 20-25, 50-55, and 80-85 were partitioned decreased by a factor of 20%, 45%, and 30%, respectively, then reassigned as new sections before subsequently being meshed.

As the sensitivity of a sensor directly corresponds to its change in amplitude for a specific mode across both damaged and undamaged beam conditions, this difference can be used to verify the contribution of a given sensor to information pertaining to a given mode under damage. When given a select arrangement of OSL, the discrepancy of modal data provided by each sensor should be sufficient to ascertain whether the proposed OSL is viable under these specific conditions.

[77] (S.K. Panigrahi, 2009)

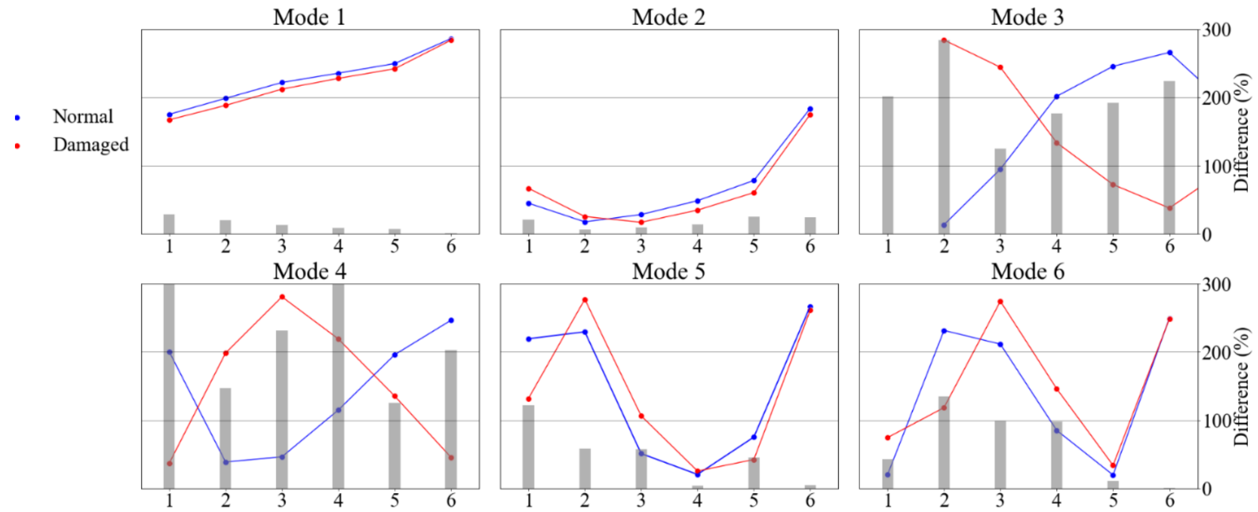

Figure 12 – Damaged beam OSL discrepancy validation for the cantilever beam

Figure 12 illustrates the information sensitivity for each sensor when applying the respective strategies in Section 6.1, decomposed for each vibration mode. Normalised amplitudes from the undamaged beam are plotted in blue, with the amplitudes from the damaged FEA model in red. The bars express the discrepancy, which is shown as a percentage difference for each sensor position.

Using the EVP/DE, significant damage information is contributed by the third and fourth vibration modes. In these, significant discrepancies in the mode shape are evident, leading most sensors to identify a change of greater than 100%. Very minor differences are observed in modes 1 and 2 across all sensors, as the normal mode shape closely mirrors the damaged state. The most considerable differences were found in mode 4, with sensors 1 and 4 reporting a 309.8% and 318.8% difference, respectively, where antinode inversion is present.

Despite this, most sensors across all modes OSLs can identify a difference of at least 10%, which exceeds most expected environmental noise contributions and sensor deviations. Most significantly, OSL clearly avoids vibration nodes, implying these strategies are successful at identifying degrees of freedom contributing to low linear independence. Though EVP may not be the most conclusive strategy when regarding individual vibration modes, when accounting for contributions of higher modes, the resulting OSL is capable of distinguishing damage.

Discrepancies do not appear to correlate to regions of stiffness reductions. Sensor 6, despite being located at element 83, where a stiffness reduction is present, only experiences a change of 1.61% and 1.02% in modes 1 and 6, respectively. This shows the investigated methodology is unable to perform Class II evaluation. Additional verification is still required, via alternative methods, such as using a Stiffness Reduction Factor (SRF) metric[26], or the use of contribution-weighing algorithms to discern between sensor differences for a specific mode, as each vibration mode is affected independently.

In spite of this, the SPO methodologies selected are acceptable as a viable strategy for SHM within the particular structure and the proposed layout can be applicable to more generalised problems of similar dimensionality.

6.3 Future Considerations

Although this study accepts these strategies as a contribution towards SHM, the field remains extensive, and many improvements can be developed or focused on the field of VDD SHM. The scope of this study was heavily limited to Class I data-based VDD of an elastic beam under purely flexural vibration. Future work should consider the methods applicable to other materials, specifically composites. Further development of early damage detection algorithms should be robust to generalise to more complex damage modes. Impact damage, fibre breakage, and voids are some examples of such, which are consequences of the heterogeneous nature of composite materials[23]. The primary limitation of this study was the acquisition of only FEA-modelled data and artificially imposed conditions. In lieu, physical VDD and SHM should be carried out to verify the degree of accuracy achieved by the OSL over progressive fatigue, providing insight into other external conditions unaccounted for. The physical characteristics of the sensors are a notable example - where FEA omits the contributions of weight and measurement noise; it is an unavoidable consequence of experimental evaluation.

The use of ambient vibration modal and natural frequency data is a widespread method to extract structural health information due to their ease of acquisition and extraction. However, they present certain limitations; extensive data storage is required to store vibration data of complex structures, and the method necessitates baseline data of a healthy model to compare with. Furthermore, these properties are vulnerable to some conditions within composite structures where closely situated eigenvalues can cause information extraction to be difficult[78]. A combination of more methods or a comparison between more advanced NDT approaches, such as the family of Wavelet Transformation (WT), may provide information to improving VDD within SHM[79].

Objective functions themselves should be studied independently. Despite multiple papers demonstrating overall efficiency across all methods, with some identifying EI's discrepancies, especially under noise[72], most papers do not distinguish between methods that perform more effectively. This paper discussed each metric's resilience towards a set level of Gaussian noise. Subsequent experimentation may place objective functions under varying levels of noise within a frequency domain or employing a noise distribution model more akin to that of sensor noise. Other popular strategies to consider include the families of energy-based, for instance, Kinetic Energy (KE); sensitivity-based, such as by Sun et al.[80]; and information-based, such as Information Entropy (IE)[81].

Alternatively, variants of SPO metrics could be an option, following the direction of Liu et al.[38] to a greater scale. This paper presented the use of two metrics in conjunction, namely in EI-DPV. It stands to reason the indispositions of Effective Independence may be mitigated through the combination of other strategies. EI-mass, introduced by Garvey et al.,[82] applied a mass matrix weight to the information matrix using Guyan reduction.

In a similar manner to objective functions, each OA will have advantages and drawbacks, and performance benchmarks will differ between studies and the problem[44]. The conclusion of DE as the best OA is only appropriate for this study and cannot be generalised[44]. The performance of any OA should ideally be applied over a number of design functions[83], and with their variants in mind.

Regarding such, a major complication was the choice of each OA's hyperparameter. As the choice of parameter will will influence the performance of each OA to differing degrees. Thorough literature review will provide static coefficients as estimates based on the problem's dimensionality; however, will always fall short of adaptive parameters, which actively account for the population's situation at the current iteration. If no limit for complexity was to be considered for continued study, variants of each algorithm may be explored in greater depth. A remark could also be directed regarding the ambiguity of the chosen termination criteria. Here, the report selects a combination of direct termination criteria[70]. The hybridisation alongside different criteria classes, such as derived termination or operator-based termination, could be ideal for accelerating convergence while guaranteeing termination after a finite set of iterations[69].

Despite the study showing inconsistent OSL results for GA and more intensive algorithm-specific hyperparameter tuning processes, it has proven efficiency in higher dimensionality problems[10]. More careful consideration of the GA operators, specifically the repopulation methods such as Delete-*n* or Steady-state replacement[51] may prove more beneficial in biasing the exploitation level. Alternatively, recombination methods that produce high-quality offspring may improve the consistency. An example of this includes Back-Controlled Selection (BSCO), as proposed by Kaya[84].

The number of sensors is the lower bound – the minimum possible number of sensors needed to retain complete parameter estimation. When more sensors are available, the optimisation problem's dimensionality increases, affecting the tendency for premature convergence to local solutions[85]. In GA, the order of computation scales marginally less than in DE and PSO, which supports evidence of GA outperforming either function in more complex structures. To improve the performance of DE/PSO with higher degrees of modality, heterogeneous[86] population or niching[87] variants may be introduced to facilitate multi-modal searching.

When validating with the artificially imposed damage, the study concludes the OSL can achieve Class I identification, i.e. the OSL can discern the presence of damage. However, a stiffness reduction of 20 – 40% as used is undoubtedly significant and is likely to lead to imminent failure in practical applications before diagnosis. Although a recommendation by G.M. Rowe and M.G. Bouldin[88] assesses fatigue failure to be defined at 50%, this number is a simplification of numerous internal mechanisms affecting the propagation of damage within materials. Moreover, this seldom accounts for other failure methods in structural beams[89]. Using EI-DPV in the bounded beam shows more deterministic results.

With more rigorous investigations performed and refinement of methodology and discrepancies, a more reliable means for Class II damage evaluation[6] is attainable, improving the applicability of SPO-based VDD systems in industrial SHM setting.

[78] (S. Hassani M. M., Minimizing Noise Effects in Structural Health Monitoring Using Hilbert Transform of the Condensed FRF, 2021)
[79] (C. Surace, 1994)
[80] (X. Sun, 2013)
[81] (S. Ye, 2012)
[82] (S.D. Garvey, 1996)
[83] (S. Gupta, 2021)
[84] (Kaya, 2011)
[85] (R.V. Rao V. S., 2011)
[86] (P. Pongchairerks, 2005)
[87] (R. Brits, 2002)
[88] (G.M Rowe, 2000)
[89] (N. Zimmermann, 2020)

References

A. Alajmi, J. W. (2014). Selecting the Most Efficient Genetic Algorithm Sets in Solving Unconstrained Building Optimization Problem. *Internation Journal of Sustainable Built Environment, Vol. 3*, 18-26.

A. Pandey, M. B. (1991). Damage Detection from Changes in Curvature Mode Shapes. *Journal of Sound Vibration, Vol.145*, 321-332.

A. R. Rao, K. L. (2014). A Generalized Optimal Sensor Placement Technique for Structural Health Monitoring and System Identification. *Procedia Eng, Vol. 86*, 529-538.

ABAQUS, Inc. (2009). *Natural Frequency Extraction, Section 6.3.5.* Retrieved from ABAQUS Analysis User's Manual, Version 6.6: https://classes.engineering.wustl.edu/

Allemang, R. (1982). A Correlation Coefficient for Modal Vector Analysis. *Proceedings of the 1st International Modal Analysis Conference*, 110-116.

Andrés, L. S. (2008). *MEEN 617 - HD#7 Undamped Modal Analysis of MDOF Systems.* Retrieved from https://rotorlab.tamu.edu/

B. Alhijawi, A. A. (2023). Genetic Algorithms: Theory, Genetic Operators, Solutions, and Applications. In A. A. B. Alhijawi, *Evolutionary* .

B. Bhattacharyya, S. G. (2007). Reactive Power Optimization through Evolution Techniques: A Comparative Study of the GA,DE, and PSO. In *Intelligent Automation and Soft Computing Vol. 13 No. 4* (pp. 453-461). Kolkata.

B. Jain, H. P. (2001). *On Termination Criteria of Evolutionary Algorithms.*

B. Shi, M. C. (2022). A Directional Continuous Wavelet Transform of Mode Shape for Line-Type Damage Detection in Plate-Type Structures. *Mechacnical System and Signal Processing, Vol. 167*, 1-24.

B.T. Svendsen, G. F. (2022, Vol.12). A Data-based Structural Health Monitoring Approach for Damage Detection in Steel Bridges Using Experimental Data. *Journal of Civial Structural Health Monitoring*, 101-115.

Baudin, M. (2011). *Introduction to Unconstrained Optimization.*

Boashash, B. (2016). Part I: A Time-Frequency Tutorial. In *Time-Frequency Signal Analysis.*

Booker, I. (1987). Improving Search in Genetic Algorithms. *Genetic Algorithms and Stimulated Annealing*, 61-73.

Boyd, S., & Bandenberghe, L. (2004). Convex Optimization. In S. Boyd, *Convex Optimization.* Cambridge University Press .

Brownjohn, J. (2007). Sturctural Health Monitoring of Civil Infrastructure. *Philos T Roy Soc, Vol. 365*, 589-622.

C. Surace, R. R. (1994). Crack Detection of a Beam Using the Wavelet Transform. *Proc. SPIE*, 1141-1147.

C.R. Farrar, G. J. (1997). System Identificatrion from Ambient Vibration Measurements on a Bridge. *Journal, Vol.205*, 1-18.

Cawley, P., & Adams, R. D. (1979). The Location of Defects in Structures from Measurements of Natural Frequencies. *Strain Anal. Eng. Des.*

Clerc, M. a. (2002). The Particle Swarm — Explosion, Stability, and Convergence in a Multidimensional Complex Space. *IEEE Transactions on Evolutionary Computation 6, No. 1*, 58–73.

D. Bhandari, C. M. (2012). Variance as a Stopping Criterion for Genetic Algorithms with an Elitist Model. *Fundamenta Informaticae 120*, 145-164.

D.C. Kammer, M. T. (2004). Optimal Placement of Triaxial Accelerometers for Modal Vibration Tests. *Mechanical System Signal Processing, Vol. 18*, 29-41.

E.L. Lehmann, G. C. (1998). *Theory of Point Estimation.*

F. Frigui, J. F. (2018). Global Methodology for Damage Detection and Localization in Civil Engineering Structures. *Engineering Structures, Vol. 171*, 686-695.

F.E. Udwadia, J. G. (1985). Optimal Sensor Locations for Structural Identification. *JPL Proceedings of the Workshop on Identification and Control of Flexible Space Structures*, 247-261.

G. Ferreira Gomes, S. d. (2018). Sensor Placement Optimization Applied to Laminated Composite Plates under Vibration. *Structural and Multidiscplinary Optimization, Vol.58*, 2099-2118.

G. Pasch, S. W. (2022). Enhanced Method for Optimum Driving Point Identification for Modal Testing. *Journal of Vibration and Control, Vol. 0*, 1-12.

G.F. Gomes, Y. M. (2018). A Numerical-Experimental Study for Structural Damage Detection in CFRP Plates Using Remote Vibration Measurements. *Journal of Civil Structural Health Monitoring, Vol. 8*, 33-47.

G.M Rowe, M. B. (2000). *Improved Techniques to Evaluate the Fatigue Resistance of Asphaltic Mixtures.*

Guimei Gu, Y. Z. (2016). *Optimal Layout of Sensors on Wind Turbine Blade Based on Combinational Algorithm.*

H. Hao, M. A. (2002). Vibration-based Damage Detectino of Structures by Genetic Algorithm. *Journal of Computing in Civil Engineering, Vol.16*, 222-229.

I. Ahmandianfar, A. S.-K.-H. (2017). Extracting Optimal Policies of Hydropower Multi-Reservoir Systems Utilizing Enhanced Differential Evolution Algorithm. *Water Resources Management Vol.31*, 4375-4397.

J. Vesterstrøm, R. T. (2004). A Comparative Study of Differential Evolution, Particle Swarm Optimization, and Evolutionary Algorithms on Numerical Benchmark Problems. *Proceedings of the 2004 Congress on Evolutionary Computation IEEE*, 1980-1987.

John, H. (1975). *Adaptation in Natural and Artifical Systems.*

K. Yeh, X. T. (1988). Uniform Strength Design of Beams with Non-zero Minimum Flexural Rigidty under Multiple Loadings. *Applied Mathematical Mechanics, Vol. 9*, 113-122.

K.F. Man, K. T. (1996). Genetic Algorithms: Concepts and Applications. *IEEE Transactions of Industrial Electronics, Vol.43, No. 5*, 519-534.

Kammer, D. C. (1991). Sensor Placement for On-Orbit Modal Identification and Correlation of Large Space Structures. *University of Wisconsin, Madison, WI 53706*, 2984-2986.

Kang Liu, R.-J. Y. (2018). Optimal Sensor Placement and Assessmnt for Modal Identificaiton. *Ocean Engineering, Vol. 165*, 209-220.

Kaya, M. (2011). The Efects of Two New Crossover Operators on Genetic Algorithm Performance, Volume 11. In *Applied Soft Computing* (pp. 881-890).

Krishnanunni, C. (2019). Sensitivty-based Damage Detection Algorithm for Structues Using Vibration Data. *Journal of Civil Structural Health Monitoring 9*, 137-143.

L. Le Letty, A. L. (1978). Optimization of Sensor Locations in Distributed Parameter System Identification. *Identification and System Parameter Estimation*, 1581-1592.

M. Civera, M. L. (2021). A Multi-objective Genetic Algorithm Strategy for Robust Optimal Sensor Placement. *Computer-Aided Civil and Infrastructure Engineering, Vol. 36*, 1185-1202.

M. Georgioudakis, V. P. (2020). A Comparative Study of Differential Evolution Variants in Constrained Structural Optimization. *Computational Methods in Structural Engineering, Vol. 6*.

M. Leon, N. X. (2014). Investigation of Mutation Strategies in Differential Evolution for Solving Global Optimization Problems. In *Artifical Intelligence and Soft Computing* (pp. 371-383).

M. Meo, G. Z. (2004). On the Optimal Sensor Placement Techniques for a Bridge Structure. *Engineering Structures 27*, 1488-1497.

M. Wang, N. L. (2021). High-Sensitive Flexural Sensors for Health Monitoring of Composite Materials Using Embedded Carbon Nanotube (CNT) Buckypaper. *Composite Structures Vol. 261*, 1-13.

N. Zimmermann, P. H. (2020). A Review of Failure Modes and Fracture Analysis of Aircraft Composite Materials. *Engineering Failure Analysis, Vol. 115*, 1-13.

Naumann, S. (2021). *Piezeoresistive Sensing Approaches for Structural Health Monitoring of Polymer Composites - A Review.*

O. Roeva, S. F. (2013). *Influence of the Population Size on the Genetic Algorithm Performance in Case of Cultivation Process Modelling.*

P. Chauhan, K. D. (2013). Novel Inertia Weight Strategies for Particle Swarm Optimization. *Memetic Computing, Vol. 5*, 229-251.

P. Gao, K. L. (2021). *Quantum Second-Order Optimization Algorithm for General Polynomials.*

P. Pongchairerks, V. K. (2005). A Non-homogenous Particle Swarm Optimization with Multiple Social Structures. *Proceedings of the International Conference on Simulation and Modelling*.

Qatar, C. M. (n.d.). *Particle Swarm Optimization 312-341*. Retrieved from pso-book-extract: https://web2.qatar.cmu.edu/~gdicaro/15382-Spring18/hw/hw3-files/pso-book-extract.pdf

R. Brits, A. E. (2002). A Niching Particle Swarm Optimizer. *Conference on Simulated Evolutions and Learning*, 692-696.

R. Eberhart, J. K. (1995). A New Optimizer Using Particle Swarm Theory. *MHS'95 Proceedings of the Sixth International Symposium on Micro Machine and Human Science*, 39-43.

R. Storn, K. P. (1996). *Differential Evolution - A Simple and Efficient Adaptive Scheme for Global Optimization over Continuous Spaces.*

R.D. Adams, P. C. (1978). A Vibration Technique for Non-Destrubtively Assessing the Integrity of Structures. *Journal of Mechanical Engineering Science, Vol. 20*.

R.N. Greenwell, J. A. (1995). Optimal Mutation Probability for Genetic Algorithms. *Mathl. Comput. Modelling Vol.21*, 1-11.

R.V. Rao, H. K. (2018). Multi-Team Perturbation Guiding Jaya Algorithm for Optimization of Wind Farm Layout. *Applied Soft Computing Journal 71*, 800-815.

R.V. Rao, V. S. (2011). Teaching-Learning Based Optimiation: A Novel Method for Constrained Mechanical Design Optimization Problems. *Copmuter-Aided Design 43, Vol.3*, 303-315.

S. Ghoreishi, A. C. (2017). Termination Criteria in Evolutionary Algorithms: A Survey. *Proceedings of the 9th International Joint Conference on Computational Intelligence IJCCI*, 373-384.

S. Gopalakrishnan, M. R. (2011). Computational Techniques for Damage Detection, Classification and Quantification. *Computational Techniques for Structural Health Monitoring*, 407-461.

S. Gupta, H. A. (2021). Comparison of Metaheuristic Optimization Algorithms for Solving Constrained Mechanical Design Optimization Problems. *Expert Systems with Applications, Vol. 183*.

S. Hassani, M. M. (2021). Minimizing Noise Effects in Structural Health Monitoring Using Hilbert Transform of the Condensed FRF. *Proceedings of the 13th International Workshop on Structural Health Monitoring, IWSHM 2021,*, 915-922.

S. Hassani, M. M. (2022). Structural Health Monitoring in Composite Structures: A Comprehensive Review. *Sensors, Vol. 22*.

S. Hassani, U. D. (2023). *A Systematic Review of Optimization Algorithms for Structural Health Monitoring and Optimal Sensor Placement.*

S. Katoch, S. C. (2020). A Review on Genetic Algorithm: Past, Present, and Future. In *Multimedia Tools and Applications* (pp. 8091-8126).

S. Mustapha, Y. L.-T. (2021). Sensor Networks for Structures Health Monitoring: Placement, Implementations, and Challenges - A Review. *Vibration,Vol. 4*, 551-585.

S. Omatu, S. K. (1978). Optimal Sensor Location for Linear Distributed Parameter Systems. *IEEE Transactions on Automatic Control, Vol. AC-23, No.4*, 665-673.

S. Padula, D. P. (1998). Optimal Sensor/Actuator Locations for Active Structural Acoustic Control. *Proceedings of the 39th AIAA/ASME/ASCE/AHS/ASC Structures, Structural Dynmaics, and Materials Conference and Exhibit*, 1865.

S. Ye, Y. N. (2012). Information Entropy Based Algorithm of Sensor Placement Optimization for Structural Damage Detection. *Smart Structure Systems. Vol. 10*, 443-458.

S.D. Garvey, M. F. (1996). Evaluation of a Method of Automatic Selection of Measurement Locations Based on Subspace-Matching. *Proceedings of SPIE - The International Society for Optical Engineering, Vol. 2768*, 1546-1552.

S.K. Panigrahi, S. C. (2009). Vibration-based Damage Detection in a Uniform Strength Beam Using Genetic Algorithm. *Meccanica, Vol.44*, 697-710.

Sastry K, G. D. (2014). Search Methologies. In *Genetic Algorithms* (pp. 93-117).

T. Marawala, S. C. (2006). Fault Classification in Structures with Incomplete Measured Data using Auto Associvative Neural Networks and Genetic Algorithm. *Curr Sci, Vol. 90*, 542-548.

Thomas Industry. (2022). *Types of Structural Steel Shapes and Beams*. Retrieved from Thomasnet: https://www.thomasnet.com/articles/metals-metal-products/types-of-steel-beams-and-shapes/

V.M. Karbhari, F. A. (2009). *Structural Health Monitoring of Civil Infrastructure Systems.*

Vijendra Kumar, S. Y. (2022). A State-of-the-Art Review of Heuristic and Metaheuristic Optimization Techniques for the Management of Water Resources. *Water Supply 22, Vol.4*, 3702-3728.

W. Fan, P. Q. (2011). Vibration-based Damage Identification Methods: A Review and Comparative Study. *Sturctural Health Monitoring, Vol. 10*, 83-111.

W. Gong, Z. C. (2013). Differential Evolution with Ranking-Based Mutation Operators. *IEEE Transactions on Cybernetics. Vol. PP*, 1-16.

W. L. Poston, R. T. (1992). Maximizing the Determinant of the Information Matrix with the Effective Independence Method. *Journal of Guidance, Control, and Dynamics, Vol.15, No.6*, 1513-1514.

W. Ostachowicz, R. S. (2019). Optimization of Sensor Placement for Structural Health Monitoring: A Review. *Structural Health Monitoring, Vol. 18*.

Wei Li, G.-G. W. (2021). A Survey of Learning-Based Intelligent Optimization Algorithms. In G.-G. W. Wei Li, *A Survey of Learning-Based Intelligent Optimization Algorithms* (pp. Volume 28, 3781-3799).

Whitworth, H. (2000). Evaluation of the Residual Strength Degradation in Composite Laminates Under Fatigue Loading. *Composite Structures, Vol. 48*, 261-264.

Wright, A. (1991). Genetic Algorithms for Real Parameter Optimization. *Foundations of Genetic Algorithms*.

X. Sun, G. H. (2013). Sensitivity-based Optimal Sensor Placement of Multi-type Sensor. *Health Monitoring of Structural and Biological Systems, Vol. 8695*, 924-933.

X. Ye, K. W. (2012). Statistical Analysis of Stress Spectra for Fatigue Life Assessment of Steel Bridges with Structural Health Monitoring Data. *Engineering Structures. Vol.45*, 166-176.

X. Yu, M. G. (2010). *Introduction to Evolutionary Algorithms.*

Y. Li, Y. C. (2019). Niching Particle Swarm Optimization with Equilibrium Factor for Multi-Modal Optimization. *Information Sciences, Vol. 494*, 233-246.

Y. Shi, R. E. (1998). A Modified Particle Swarm Optimizer. *IEEE International Conference on Evolutionary Computational Intelligence*, 69-73.

Y. Tan, L. Z. (2019). Computational Methodologies for Optimal Sensor Placement in Structural Health Monitoring: A Review. *Sturctural Health Monitoring, Vol.19*, 1287-1308.

Y. Wang, Z. T. (2021). Differential Evolution with Adaptive Mutation Strategy Based on Fitness Landscape Analysis. *Information Sciences, Vol. 549*, 142-163.

Y.Q. Ni, A., Ye, X. W., & J.M. Ko, F. (2010). *Monitoring-Based Fatigue Reliability Assessment of Steel Bridges: Analytical Model and Application.*

Z. H. Qureshi, T. S. (1980). Optimum Experimental Design for Identification of Distributed Parameter Systems. *International Journal of Control, Vol. 31, No. 1*, 21-29.